ACES Asian Chemical Editorial Society

DOI: 10.1002/cnma.201800186

CHEMNANOMAT Communication

Supramolecular Polymers

SPECIAL ISSUE

Synergy of Axial and Point Chirality to Construct Helical *N*-Heterotriangulene-Based Supramolecular Polymers

Yeray Dorca,[a] Jorge S. Valera,[a] Jesús Cerdá,[b] Juan Aragó,[b] Rafael Gómez,[a] Enrique Ortí,*[b] and Luis Sánchez*[a]

Abstract: We report on the cooperative supramolecular polymerization of a series of *N*-heterotriangulenes that aggregate into helical columnar stacks by the operation of H-bonding interactions between the peripheral amide groups and π-stacking of the central aromatic moieties. The helical outcome of the highly stable supramolecular polymers stems from the joint effect of the point chirality dictated by the stereogenic centers at the side chains that, in turn, conditions the molecular atropisomerism generated by the restricted rotation of the peripheral benzamide moieties affording a propeller-like geometry. To the best of our knowledge, this is the first example in which two different elements of asymmetry act together to bias the helicity of chiral supramolecular polymers.

Helical structures are inherently chiral entities amply present in Nature. DNA, proteins and polysaccharides exemplify the complexity reached by helical biopolymers that are responsible for extremely relevant functions.[1] The binomial helicity-functionality has prompted the scientific community to the quest of new helical macromolecules that emulate these naturally occurring complex and functional structures, especially in the field of covalent polymers.[2] Supramolecular polymers are also being elegantly exploited as materials with improved mechanical, biomimetic and optoelectronic applications.[3] Supramolecular polymerization is, indeed, an excellent strategy to construct helical entities.[4] A vast majority of helical supramolecular polymers are generated by the efficient transmission of the chiral information associated with the stereogenic centers at peripheral side chains.[4,5] Helicity can be also induced by the presence of axial chirality in the molecular building blocks. In these examples, this element of asymmetry dominates the helical outcome of the supramolecular polymer regardless the presence of point chirality.[6]

Herein, we describe the cooperative supramolecular polymerization of *N*-heterotriangulenes **1–3** (Figure 1a), which self-assemble to yield highly stable helical aggregates. *N*-heterotriangulenes (NHTs) are known to form helical supramolecular structures exhibiting excitation energy transport over more than 4 μm.[7,8] In the case of NHTs **1–3**, the final helical outcome is dictated by the synergy of both molecular atropisomerism, generated by the restricted rotation of the peripheral benzamide moieties that affords a propeller-like geometry (Figure 1b), and the point chirality embedded in the side chains. To the best of our knowledge, this is the first example in which the synergy of both axial and point chirality is responsible for the construction of helical supramolecular polymers (Figure 1c). The results presented in this manuscript shed light on the contribution of the different elements of molecular asymmetry to bias the hierarchical organization of self-assembling units into helical aggregates.

The synthesis of **1–3** was performed by following previously reported protocols in which the Suzuki cross-coupling between the corresponding 4-(alkylcarbamoyl)phenyl boronic acid and the triiodo-NHT core is the final step (Scheme S1). All the novel compounds were fully characterized using the standard spectroscopic and spectrometry techniques (see the Supporting Information).

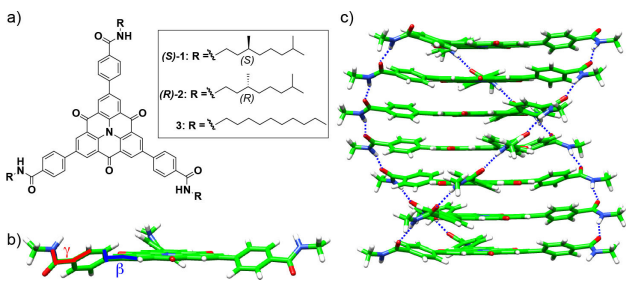

Figure 1. a) Chemical structure of NHTs ***(S)*-1**, ***(R)*-2** and achiral **3**. b) Minimum-energy structure calculated for one of the two possible atropisomers of the monomer NHT model used to simulate systems **1**–**3**. c) Right-handed helical columnar arrangement of a heptamer of the NHT model. The blue and red lines in (b) depict the torsional angles formed by the benzamide unit and the *N*-heterotriangulene core (β) and the benzene ring and the amide functional group (γ), respectively. The blue dotted lines in (c) depict the triple array of H-bonds established between the amide groups.

[a] *Y. Dorca, J. S. Valera, Dr. R. Gómez, Prof. Dr. L. Sánchez*
Departamento de Química Orgánica I
Facultad de Ciencias Químicas, UCM
Ciudad Universitaria, s/n, 28040, Madrid (Spain)
E-mail: lusamar@quim.ucm.es
[b] *J. Cerdá, Dr. J. Aragó, Prof. Dr. E. Ortí*
Instituto de Ciencia Molecular
Universidad de Valencia, 46980 Paterna (Spain)
E-mail: enrique.orti@uv.es

Supporting information for this article is available on the WWW under https://doi.org/10.1002/cnma.201800186

This manuscript is part of a Special Issue on Supramolecular Nanostructures. Click here to see the Table of Contents of the special issue.

The C_3 symmetry of compounds **1–3** and the presence of the amide functional groups are design principles that should favour an efficient helical self-assembly by the formation of a triple array of intermolecular H-bonding interactions and the π-stacking of the aromatic NHT cores.[8,9] The ^{1}H NMR spectra of **1–3** in $CDCl_3$ show broad resonances diagnostic of the strong tendency that **1–3** have to aggregate (Figure 2a and S1). The complete spectroscopic characterization of the reported compounds can only be achieved by registering the ^{1}H NMR spectra in a solvent like THF-d8, which competes for the formation of H-bonds and provides well-defined resonances. FTIR spectroscopy further corroborates the supramolecular interaction of **1–3** by H-bonding interactions. The FTIR spectra show the N–H and Amide I (C=O) stretching bands at ~3270 and ~1660 cm^{-1}, respectively. In addition, the Amide II (C–N) bending band is observed at ~1545 cm^{-1} (Figure S2). These wavenumbers are associated with an α-helix arrangement of the stacked molecules by the operation of a triple array of H-bonds.[9,10]

The helical supramolecular arrangement is supported by density functional theory (DFT) and DFT tight-binding (DFTB) calculations at the B3LYP-D3/6-31G** and SCC-DFTB level, respectively (see the theoretical section in the Supporting Information). Calculations show that the monomer model of **1–3**, where the alkyl chains have been replaced by methyl groups, exhibits a planar carbonyl-bridged triphenylamine NHT core with the peripheral benzamide units rotated 34° (angle β in Figure 1b) conferring the molecule a propeller-like shape. This propeller-like structure effectively aggregates into a helical columnar stack governed by H-bonds and π–π interactions, where adjacent molecules are separated by 3.1 Å and rotated by 21.7° along the stacking axis (Figure 1c and S3). In this helical stack, the benzamide units are twisted by ~20° (angle β) to maximize the π–π interactions between benzene rings in adjacent molecules. The amide groups are additionally rotated by ~40° (angle γ) to optimize the triple array of H-bonding interactions along the stack with N–H···O=C distances of ~1.9 Å (Figure S13). The combination of SCC-DFTB and B3LYP–D3 calculations predict a cooperative supramolecular mechanism for the self-assembly of these *N*-heterotriangulenes. The calculated interaction energy per monomer unit ($\Delta E_{mon,n}$) shows a hyperbolic behavior with an asymptotic limit of −87.1 kcal mol^{-1} (Figure S4). The rapid growth of $\Delta E_{mon,n}$ implies an initial nucleation regime in which the stabilization of the primary aggregate increases rapidly with the number of added monomers. The asymptotic region corresponds to the elongation process in which further addition of monomeric units has no remarkable effect on the interaction energy.[11]

A detailed investigation of the supramolecular polymerization mechanism followed by **1–3** has been performed by variable temperature (VT) UV-Vis experiments. In apolar solvents like methylcyclohexane (MCH) or heptane, the studied NHTs are scarcely soluble and only the addition of a co-solvent like toluene (Tol) allows the complete solution of the aggregates and also their disassembly into molecularly dissolved species by heating at 90 °C. In good correlation with that described for related self-assembled NHTs,[8] the UV-Vis spectra of the aggregated state of **1–3**, at a total concentration (c_T) of 10 μM, show two broad bands centered at 318 and 441 nm and a shoulder at ~470 nm. Heating the samples at 90 °C results in the apparition of well defined bands at 317, 410 and 438 nm (Figure 2b and S5a). These changes are indicative of the formation of H-type aggregates.[9,12] Plotting the variation of these bands against the degree of aggregation α results in non-sigmoidal curves characteristic of a cooperative supramolecular polymerization (Figure 2c and S5b).[13] Making use of the equilibrium (EQ) model reported by Ten Eikelder et al.,[14] we have calculated the thermodynamic parameters (the enthalpy of elongation (ΔH_e), the entropy of elongation (ΔS), the nucleation penalty (ΔH_n), the nucleation (K_n) and elongation (K_e) binding constants, the cooperativity factor (σ), and the temperature at which the nucleation regime changes into the elongation one (T_e)) associated with the supramolecular polymerization mechanism of **1–3** (Figure 2c and S5b and Table 1).

Compared with related NHTs, compounds **1–3** show larger K_n and K_e constants and higher T_e values, confirming the high thermal stability and the strong tendency to form one-dimensional columnar structures of the supramolecular polymers formed by **1–3**.[8,9,15] In fact, atomic force microscopy (AFM) imaging of compound ***(R)*-2** at $c_T = 10$ μM onto mica confirms the formation of a dense network of interconnected fibrillary structures with typical heights of ~2.5 nm (Figure 3 and S6).

The helical character of the aggregates formed by the self-assembly of chiral NHTs ***(S)*-1** and ***(R)*-2** has been investigated

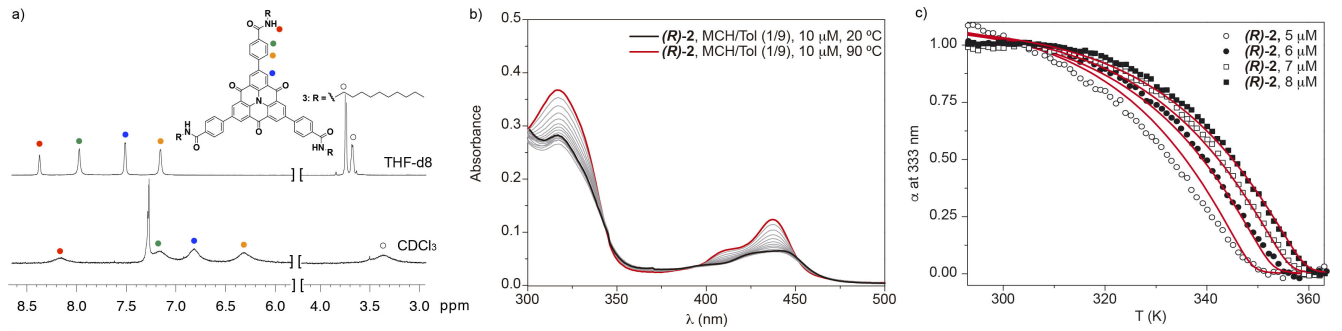

Figure 2. a) Partial ^{1}H NMR of **3** in $CDCl_3$ and THF-d8 (300 MHz, 298 K). b) Variable temperature UV-Vis spectra of ***(R)*-2** upon cooling from 90 to 20 °C at intervals of 10 °C (MCH/Tol 1/9; $c_T = 10$ μM). c) Variation of the degree of polymerisation (α) of ***(R)*-2** versus temperature cooling at 1 K min^{-1}. Red curves correspond to the fitting to the equilibrium (EQ) model.

Table 1. Thermodynamic parameters derived for the supramolecular polymerization of compounds ***(S)*-1**, ***(R)*-2** and **3** (MCH/Tol, 1/9).

Parameter[a]	***(S)*-1**	***(R)*-2**	**3**
ΔH_e [kJ mol^{-1}]	-42.4 ± 0.5	-44.3 ± 0.9	-47.2 ± 0.9
ΔS [J K mol^{-1}]	-20 ± 1	-25 ± 2	-34 ± 2
ΔH_n [kJ mol^{-1}][a]	-21.2 ± 0.7	-25.1 ± 1.7	-24.4 ± 1.7
σ[b]	19.2×10^{-5}	3.9×10^{-5}	5.1×10^{-5}
K_e [L mol^{-1}][b]	2.5×10^6	2.9×10^6	3.2×10^6
K_n [L mol^{-1}][b]	4.8×10^2	1.1×10^2	1.6×10^2
T_e [K][c]	358, 353, 347, 342	358, 355, 351, 347	358, 355, 350, 345

[a] The nucleation penalty ΔH_n is negative, which implies that the enthalpy gain is smaller for nucleation compared to elongation. [b] The equilibrium constants for elongation and dimerization, K_e and K_n, and the cooperativity factor σ ($=K_n/K_e$) are calculated at 298 K. [c] T_e values are calculated for 8, 7, 6 and 5 μM.

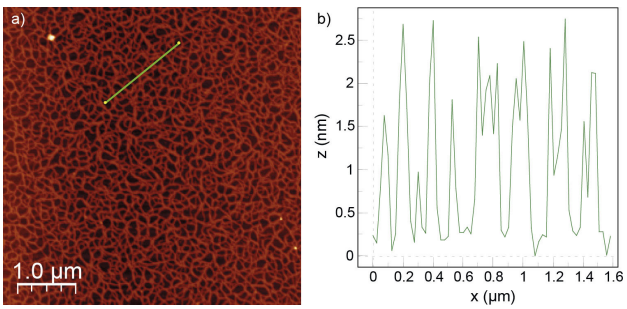

Figure 3. a) Height AFM image and b) height profile along the green line of a drop-cast solution of ***(R)*-2** in MCH/Tol (1/9) onto mica at $c_T = 10$ μM. The z scale is 12 nm.

by circular dichroism (CD). In MCH/Tol (1/9) and at $c_T = 10$ μM, compounds ***(S)*-1** and ***(R)*-2** show a rich but low intense dichroic pattern with bands at 307, 336 and 428 nm that is cancelled by heating the solution at 90 °C (Figure S7a). Increasing the concentration at $c_T = 100$ μM, the dichroic pattern increases in intensity and a new band centerd at 455 nm arises (Figure 4a). The high thermal stability of the aggregates makes that heating the 100 μM solution does not result in a total cancellation of the dichroic response. In fact, a similar dichroic pattern is obtained by using solvents like toluene, $CHCl_3$ or THF that favour the solvent-solute interactions (Figure 4b, S7b and S7c).

The dichroic pattern exhibited by ***(S)*-1** and ***(R)*-2** contrasts with that observed for referable C_3-symmetric self-assembling units that, upon supramolecular polymerization, afford a single and intense bisignate Cotton effect ascribable to the efficient transfer of the point chirality embedded in their side chains to the columnar helical aggregate.[5c,9,10,15] However, the dichroic pattern of ***(S)*-1** and ***(R)*-2** resembles that observed for supramolecular polymers formed by chiral self-assembling units possessing asymmetry elements other than point chirality.[6] These findings suggest that the helical outcome of the supramolecular polymerization of ***(S)*-1** and ***(R)*-2** stems from a synergistic effect of the atropisomerism generated by the restricted rotation of the benzamide units and the point chirality of the stereogenic centers at the peripheral side chains. This synergistic effect is only operative in the self-assembled state of both ***(S)*-1** and ***(R)*-2** since the molecularly dissolved state of these chiral units and both the aggregated and molecularly dissolved states of achiral **3** show no dichroic response (Figure S8).

To corroborate this synergistic effect on the helical outcome of the supramolecular polymerization of ***(S)*-1** and ***(R)*-2**, the dichroic response of the two possible atropisomers generated by the restricted rotation of the benzamide units was calculated at the DFT level (see the Supporting Information). The positive or negative value of angle β in the isolated monomer of the NHTs generates *M* and *P* atropisomers. The calculated CD spectra of such atropisomers display three maxima at 285, 329 and 399 nm (Figure S9). More interestingly, the computed CD spectra of the *P* and *M* dimers (Figure 4c) present the same dichroic pattern to that experimentally observed for ***(S)*-1** and ***(R)*-2**, respectively. Therefore, the point chirality embedded in the peripheral side chains conditions the formation of helical columnar stacks constituted by *P* atropisomers for ***(S)*-1** (Figure 1c) and *M* atropisomers for ***(R)*-2**.

In summary, we have reported on the self-assembly of a series of *N*-heterotriangulenes that form, cooperatively, highly stable helical supramolecular polymers. The helical outcome stems from the synergy of the point chirality dictated by the stereogenic centers at the side chains that, in turn, conditions the molecular atropisomerism generated by the restricted rotation of the peripheral benzamide moieties leading to a propeller-like geometry. To the best of our knowledge, this is

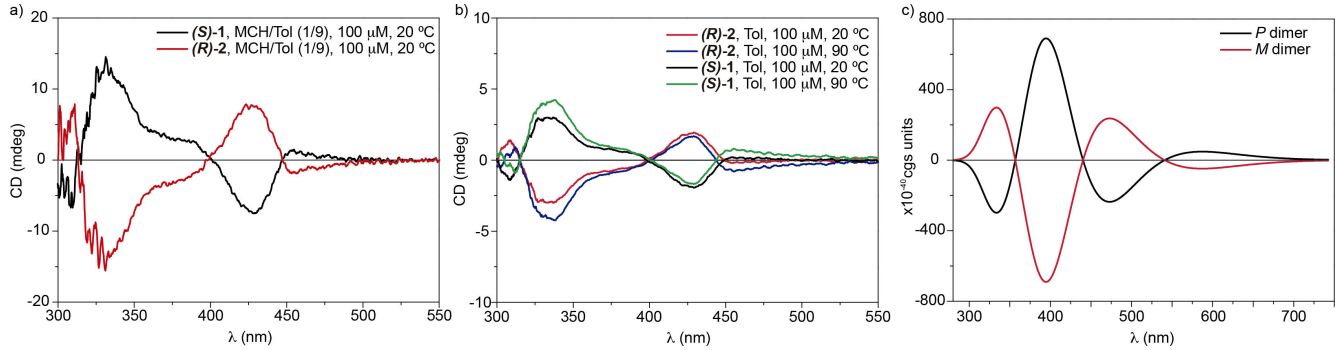

Figure 4. CD spectra of ***(S)*-1** and ***(R)*-2** in MCH/Tol (1/9) (a) and in Tol (b) at $c_T = 100$ μM. c) Theoretical simulation of the CD spectra calculated for the *P* and *M* dimers of the NHT model shown in Figure 1b.

the first example in which two different elements of asymmetry act together to bias the helicity of chiral supramolecular polymers.

Acknowledgements

Financial support by the MINECO of Spain (CTQ2014-53046-P, CTQ2015-71154-P, and Unidad de Excelencia María de Maeztu MDM-2015-0538), the Generalitat Valenciana (PROMETEO/2016/135), the Comunidad de Madrid (NanoBIOSOMA, S2013/MIT-2807), and European FEDER funds (CTQ2015-71154-P) is acknowledged. Y.D. is grateful to Comunidad de Madrid for his predoctoral fellowship. J.S.V. and J.C. are thankful to the MINECO for their FPI predoctoral fellowships. J.A. is also thankful to the MINECO for a "JdC-Incorporación" Fellowship (IJCI-2015-26154).

Conflict of Interest

The authors declare no conflict of interest.

Keywords: atropisomerism · cooperativity · helicity · point chirality · supramolecular polymers

[1] D. J. Jockhart, E. A. Winzeler, *Nature* **2000**, *405*, 827–836.
[2] a) E. Schwartz, M. Koepf, H. J. Kitto, R. J. M. Nolte, E. Rowan, *Polym. Chem.* **2011**, *2*, 33–47; b) E. Yashima, K. Maeda, H. Iida, Y. Furusho, K. Nagai, *Chem. Rev.* **2009**, *109*, 6102–6211.
[3] T. Aida, E. W. Meijer, S. I. Stupp, *Science* **2012**, *335*, 813–815.
[4] a) A. R. A. Palmans, E. W. Meijer, *Angew. Chem.* **2007**, *119*, 9106–9126; *Angew. Chem. Int. Ed.* **2007**, *46*, 8948–8968; b) M. Liu, L. Zhang, T. Wang, *Chem. Rev.* **2015**, *115,* 7304–7397.
[5] a) W. Jin, T. Fukushima, M. Niki, A. Kosaka, N. Ishii, T. Aida, *Proc. Natl. Acad. Sci. USA* **2005**, *102*, 10801–10806; b) P. Jonkheijm, P. van der Schoot, A. P. H. J. Schenning, E. W. Meijer, *Science* **2006**, *313*, 80–83; c) F. García, P. M. Viruela, E. Matesanz, E. Ortí, L. Sánchez, *Chem. Eur. J.* **2011**, *17*, 7755–7759; d) F. García, L. Sánchez, *J. Am. Chem. Soc.* **2012**, *134*, 734–742; e) M. Hifsudheen, R. K. Mishra, B. Vedhanarayanan, V. K. Praveen, A. Ajayaghosh, *Angew. Chem.* **2017**, *129,* 12808–12812; *Angew. Chem. Int. Ed.* **2017**, *56*, 12634–12638.
[6] a) B. Narayan, K. K. Bejagam, S. Balasubramanian, S. J. George, *Angew. Chem.* **2015**, *127*, 13245–13249; *Angew. Chem. Int. Ed.* **2015**, *54*, 13053–13057 ; b) Z. Xie, V. Stepanenko, K. Radacki, F. Würthner, *Chem. Eur. J.* **2012**, *18*, 7060 – 7070; c) J. Buendía, E. E. Greciano, L. Sánchez, *J. Org. Chem.* **2015**, *80*, 12444 – 12452; d) F. Aparicio, B. Nieto-Ortega, F. Nájera, F. J. Ramírez, J. T. López Navarrete, J. Casado, L. Sánchez, *Angew. Chem.* **2014**, *126*, 1397–1401; *Angew. Chem. Int. Ed.* **2014**, *53*, 1373–1377; e) J. S. Valera, R. Gómez, L. Sánchez, *Org. Lett.* **2018**, *20*, 2020–2023.
[7] A. T. Haedler, K. Kreger, A. Issac, B. Wittmann, M. Kivala, N. Hammer, J. Köhler, H.-W. Schmidt, R. Hildner, *Nature* **2015**, *253*, 196–200.
[8] a) A. T. Haedler, S. C. J. Meskers, R. H. Zha, M. Kivala, H.-W. Schmidt, E. W. Meijer, *J. Am. Chem. Soc.* **2016**, *138*, 10539–10545; b) J. S. Valera, R. Sánchez-Naya, F. J. Ramírez, J. L. Zafra, R. Gómez, J. Casado, L. Sánchez, *Chem. Eur. J.* **2017**, *23*, 11141–11146; c) J. S. Valera, R. Gómez, L. Sánchez, *Small,* **2018**, *14,* 1702437.
[9] a) F. García, L. Sánchez, *J. Am. Chem. Soc.* **2012**, *134*, 734–742; b) M. M. J. Smulders, I. A. W. Filot, J. M. A. Leenders, P. van der Schoot, A. R. A. Palmans, A. P. H. J. Schenning, E. W. Meijer, *J. Am. Chem. Soc.* **2010**, *132*, 611–619.
[10] F. García, P. A. Korevaar, A. Verlee, E. W. Meijer, A. R. A. Palmans, L. Sánchez, *Chem. Commun.* **2013**, *49*, 8674–8676.
[11] a) S. Díaz-Cabrera, Y. Dorca, J. Calbo, J. Aragó, R. Gómez, E. Ortí, L. Sánchez, *Chem. Eur. J.* **2018**, *24*, 2826–2831; b) J. Buendía, J. Calbo, F. García, J. Aragó, P. M. Viruela, E. Ortí, L. Sánchez, *Chem. Commun.* **2016**, *52*, 6907–6910.
[12] a) E. E. Greciano, B. Matarranz, L. Sánchez, *Angew. Chem. Int. Ed.* **2018**, DOI: 10.1002/anie.201801575; b) M. Lebtow, I. Helmers, V. Stepanenko, R. Q. Albuquerque, T. B. Marder, G. Fernández, *Chem. Eur. J.* **2017**, *23*, 6198–6205.
[13] T. F. A. De Greef, M. M. J. Smulders, M. Wolffs, A. P. H. J. Schenning, R. P. Sijbesma, E. W. Meijer, *Chem. Rev.* **2009**, *109*, 5687–5754.
[14] H. M. M. Ten Eikelder, A. J. Markvoort, T. F. A. de Greef, P. A. J. Hilbers, *J. Phys. Chem. B* **2012**, *116*, 5291–5301.
[15] A. Rödle, B. Ritschel, C. Meck-Lichtenfeld, V. Stepanenko, G. Fernández, *Chem. Eur. J.* **2016**, *22*, 15772–15777.

Manuscript received: April 26, 2018
Accepted Article published: June 1, 2018
Version of record online: July 6, 2018